Annu. Rev. Biophys. Biomol. Struct. 2005. 34:173–99
doi: 10.1146/annurev.biophys.34.040204.144517

First published online as a Review in Advance on January 27, 2005

MODELING WATER, THE HYDROPHOBIC EFFECT, AND ION SOLVATION

Ken A. Dill,[1] Thomas M. Truskett,[2] Vojko Vlachy,[3] and Barbara Hribar-Lee[3]

[1]*Department of Pharmaceutical Chemistry, University of California, San Francisco, California 94143-2240; email: dill@maxwell.ucsf.edu*

[2]*Department of Chemical Engineering and Institute for Theoretical Chemistry, The University of Texas at Austin, Austin, Texas 78712; email: truskett@che.utexas.edu*

[3]*Faculty of Chemistry and Chemical Technology, University of Ljubljana, 1000 Ljubljana, Slovenia; email: vojko.vlachy@fkkt.uni-lj.si, barbara.hribar@fkkt.uni-lj.si*

Key Words hydration, hydrogen bonds, Hofmeister series, statistical mechanics, molecular simulation

■ **Abstract** Water plays a central role in the structures and properties of biomolecules—proteins, nucleic acids, and membranes—and in their interactions with ligands and drugs. Over the past half century, our understanding of water has been advanced significantly owing to theoretical and computational modeling. However, like the blind men and the elephant, different models describe different aspects of water's behavior. The trend in water modeling has been toward finer-scale properties and increasing structural detail, at increasing computational expense. Recently, our labs and others have moved in the opposite direction, toward simpler physical models, focusing on more global properties—water's thermodynamics, phase diagram, and solvation properties, for example—and toward less computational expense. Simplified models can guide a better understanding of water in ways that complement what we learn from more complex models. One ultimate goal is more tractable models for computer simulations of biomolecules. This review gives a perspective from simple models on how the physical properties of water—as a pure liquid and as a solvent—derive from the geometric and hydrogen bonding properties of water.

CONTENTS

WATER HAS INTERESTING PHYSICAL PROPERTIES

Water is arguably the most important fluid on Earth. It is the most abundant liquid on Earth's surface, it influences the landscape and climates, and it plays a critical role in biology (5, 31, 85). Because of water's large heat capacity, the oceans store considerable thermal energy, acting as vast thermostats that govern the planet's temperature. The density maximum of liquid water is just above its freezing point, resulting in top-down freezing that enables life at the bottoms of rivers and lakes to survive winters. As a result of its high surface tension, water penetrates into rocks. Upon freezing, it then expands, fracturing the rocks and eventually turning them into soil.

Water has almost universal solvent action (31). Nearly all known chemical substances will dissolve in water at least to a small extent. It is one of the most corrosive substances known and yet is physiologically harmless. Water constitutes about half the weight of living cells (85), and it must be displaced from the surfaces of proteins, nucleic acids, and membranes when ligands bind or when biomolecules change conformations. The limitations in our understanding of water are largely responsible for the limitations in our ability to predict protein structures or to design drugs.

Despite its abundance, water is regarded as an unusual liquid when compared to simpler fluids such as argon (83). Although water is similar to simpler liquids in its van der Waals attractions and repulsions, water is interesting because of its ability to form hydrogen bonds and a three-dimensional tetrahedral network-like structure. Thus, compared to other liquids having the same molecular size, water is more cohesive, as indicated by its higher boiling and freezing temperatures, surface tension, and vaporization enthalpies (26). Further, it has a high dielectric constant and exists in numerous crystalline polymorphs. Liquid water's fluidity increases with increasing pressure. The mobility of H^+ and OH^- ions is higher in water than in other liquids (83).

Water also has volumetric anomalies (26, 31, 63, 83, 98). Whereas most solids are denser than their corresponding liquids, ice floats on water. Also, a typical liquid's density decreases monotonically with increasing temperature. For water, this is true at high temperatures (above 3.984°C, the temperature of maximum density). But it is not true for cold water, between 0° and 3.984°C. Cold water

gets denser upon warming. Other related anomalies include minima in the isobaric heat capacity and isothermal compressibility with temperature in the normal liquid range (at 36° and 46°C, respectively) (25).

A BRIEF HISTORY OF WATER MODELING

We focus here on modeling, the enterprise that aims to understand how water's properties are encoded within its molecular structure and energetics. Modeling water has been a large scientific undertaking. There have been several book-length reviews (9, 23, 26, 31, 40). Only a brief summary is given here.

Perhaps the earliest model of water originated from Roentgen in 1892 (9). Roentgen postulated a "mixture model," according to which liquid water consists of two kinds of molecules, liquid-like and ice-like. In 1933, Bernal & Fowler (12) concluded that the unique properties of water are due to the tetrahedral geometry of each water molecule. In 1946, Samoilov (67) proposed an interstitial model in which liquid water has the structure of ice, some of the cavities of which are filled with water molecules. Similarly, Pauling (57) suggested that liquid water is a hydrate with clathrate-like structures. Further insights came in 1951 from Pople (61), who postulated a point-charge model for the tetrahedral water molecule, whereby the four hydrogen bonds in ice are distorted or bent, rather than broken, upon melting.

In the 1960s and 1970s, as computer technology improved, there was a move toward computer simulations (32). One of the first simulations of liquid water was that of Barker & Watts in 1969 (6). Using Monte Carlo sampling with an intermolecular pair potential from Rowlinson (65), Barker & Watts calculated the energy, specific heat, and radial distribution function of liquid water. In 1972, Rahman & Stillinger used molecular dynamics simulations with a simple interaction site model proposed by Ben-Naim and Stillinger (the BNS model) (40). That model was later modified by Stillinger & Rahman (82, 84) and called the ST2 model. ST2 water is a five-site model in which four point charges are tetrahedrally distributed around the central oxygen atom. The central oxygen has a point charge and is a Lennard-Jones (LJ) interaction site. Another commonly used interaction site model is SPC water (11), in which the charges on three positively charged hydrogen interaction sites are balanced by an appropriate negative charge on the oxygen. Jorgensen has applied his transferable intermolecular potential functions (TIP) to water and other organic liquids (43, 44). The TIP water models, which originated in ST2, use three, four, or five interaction sites in TIP3P, TIP4P, and TIP5P, respectively. All these models treat water as rigid.

More complex models have also been developed. Ferguson, on the basis of the SPC potential, lifted the rigidity approximation by including bond stretching and bending terms (29). Sprik & Klein (81) have explicitly introduced the effects of polarization and many-body interactions. In their potential, the polarization center is represented as a collection of four tetrahedrally arranged charges whose values

are permitted to vary, but the sum of which is zero. Beginning in 1975 (48, 49), pair potentials for water models have also been derived from ab initio calculations. Examples include the MCY (51), CH (18), CC (16), and SHP (80) models.

The approaches described above aim to predict various properties of water solely on the basis of an energy function, i.e., on some conception of the structure of a water molecule and its interactions—energetic and entropic—with other water molecules nearby. Another approach, which has been pioneered by Chandler & Pratt and the Los Alamos group, has been hybrid models, in which experimental observables substitute for part of the theory. Pratt & Chandler (62) use the pair correlation function of liquid water as input, and the Los Alamos group (42), through a maximum entropy strategy, uses experimentally determined moments of water population distribution functions. Although those approaches have provided important insights into the behavior of water, our objective here is different. Our aim is to understand water's properties starting strictly from an energy function that is based on water's geometric and physical properties, without additional experimental inputs.

TOWARD SIMPLIFIED MODELS OF WATER

It is clear that making models ever more accurate, more detailed, and more faithful to the underlying quantum mechanics should lead to improved accuracy in computer simulations involving water. Why, then, should we be interested in simplified models? There are three reasons. First, simplified models often give insights that are not obtainable from computer simulations. For example, physical chemistry courses teach the ideal gas law, the van der Waals equation of state, the Ising model of magnetization, the Flory-Huggins theory of polymers, and other simple models not because they more accurately represent physical reality than computer simulations of more detailed models, but because the chain of logic from the model premises to conclusions is so much more transparent. Simpler models are more flexible in providing insights and illuminating concepts, and they do not require big computer resources. Simple models can unify our knowledge in the form of universal principles, such as the law of corresponding states. Second, simple models can explore a much broader range of conditions and external variables. Whereas simulating a detailed model may predict the behavior at one temperature and pressure, a simpler model can be used to study a whole phase diagram of temperatures and pressures. Third, analytical models can provide functional relationships for engineering applications and lead to improved models of greater computational efficiency. It has been noted that when detailed models of proteins in water are simulated on a 256-node computer, 255 of those nodes just simulate the water. There is a need for computationally cheaper models of water that can retain the relevant physics.

One of the simplest models was introduced by Ben-Naim in 1971 (8). In Ben-Naim's model, each water molecule is represented as a two-dimensional disk that interacts with other waters through a LJ interaction and an orientation-dependent

hydrogen bonding interaction. Three-dimensional simplified models have also been developed (13, 21, 75). Overviews are given by Guillot (32) and by Nezbeda (55).

The Mercedes-Benz Model Is a Two-Dimensional Version of Water

We focus here on two models. Both are two-dimensional and derive from Ben-Naim's model cited above (8). Figure 1*a* shows the Mercedes-Benz (MB) model of water, so named because of the resemblance of each water molecule to the Mercedes-Benz logo. Each water molecule is a two-dimensional disk with three radial arms (72).

In the MB model, the energy of interaction between two water molecules is the sum of a LJ attraction and repulsion and an orientation-dependent hydrogen bond interaction. Neighboring water molecules form an explicit hydrogen bond when an arm of one water molecule aligns with an arm of another water molecule; the corresponding energy is a Gaussian function of both separation and angle. Hydrogen bonding arms are not distinguished as donors or acceptors. The strength of a hydrogen bond is determined only by the degree of alignment of arms on two neighboring waters (72). The LJ interaction energy, ε_{LJ}, is set to be one tenth of the hydrogen bond energy, ε_{HB}. Also, the LJ contact distance is 0.7 of that of hydrogen bond length (72). The MB model has been studied extensively by Monte Carlo (NPT) simulations (36, 70–74, 76–78).

Simulations of this two-dimensional model are much less expensive than computer simulations of detailed three-dimensional models. A three-dimensional box of eight molecules on a side contains $8 \times 8 \times 8 = 512$ molecules, whereas a two-dimensional box contains only 64 waters. One result is that in three dimensions, computational modeling is unable to reversibly freeze water because simulations get stuck in deep kinetic traps, whereas reversible freezing and melting are readily studied in the two-dimensional MB model.

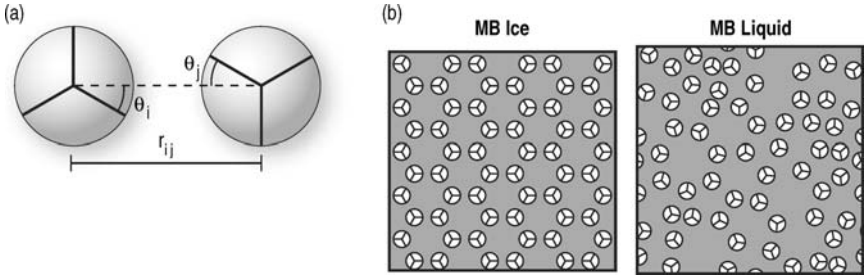

Figure 1 (*a*) MB water model. Each water is a LJ disk, with three hydrogen bonding arms. (*b*) (*Left*) MB ice, the stable state at low temperature. (*Right*) A typical liquid configuration at $T^* = 0.20$, density $\rho^* = 0.9$ (72).

This review summarizes evidence that many of water's interesting properties are not so much due to its three-dimensionality, its tetrahedrality, or its atomic details. Rather, many of water's properties follow from the relatively rigid geometric relationship among the hydrogen bonding orientations within each water molecule, much of which can be captured even in simplified two-dimensional models.

We now describe the simple insights that the MB model gives into the properties of pure water. Figure 1*b* shows the reversible freezing of MB "ice." MB ice has a hexagonal arrangement of six waters because of the symmetry dictated by the hydrogen bonding interactions. MB ice forms spontaneously from a random initial state in constant-pressure MC simulations when the temperature is low enough ($T^* = 0.14$) (72). MB ice is stable at low temperatures because hydrogen bonding is the dominant attraction—it is an order of magnitude stronger than the van der Waals interactions. Water forms hexagonal structures in two dimensions (tetrahedral structures in three dimensions) to maximize hydrogen bonding. The hexagons have lower density than if water structure were dominated by its van der Waals interactions (Figure 1).

The tendency of water to expand upon freezing shows up in the pressure-temperature phase diagram. Figure 2 compares two materials. For simple materials (left), the slope of the solid-liquid phase boundary is positive, indicating that applying pressure squeezes a normal liquid into a solid. However, for water, the solid-liquid phase boundary slope is negative, implying that applying pressure has the opposite effect: squeezing ice melts it. It is commonly argued that this pressure-induced melting is the basis for ice-skating. The pressure of the skate blade melts the ice beneath it, creating a low-friction region of water on which the skater slides. You cannot ice-skate on most other solids, such as iron. It is readily shown by the Clapeyron relation that the negative slope of the phase boundary follows directly for any material having a solid that is less dense than its liquid:

$$\frac{dp}{dT} = \frac{\Delta h}{T\,\Delta V}. \qquad 1.$$

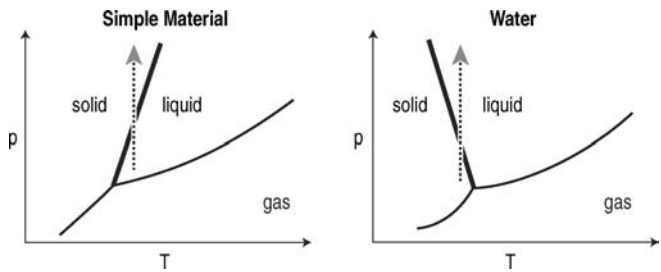

Figure 2 Pressure-temperature phase diagram for a typical simple liquid (*left*) and water (*right*). Pressure melts typical solids, but pressure freezes water (25).

(A well-known caveat is that the pressures required for ice-skating are somewhat lower than those predicted from the equation above, presumably owing to less structuring in surface waters.) The MB model is consistent with such experiments and gives a negatively sloped phase boundary between the liquid and solid phases because its solid is less dense than its liquid.

The MB model qualitatively predicts the unusual properties of pure water, including the density anomaly, the minimum in the isothermal compressibility, and a large heat capacity (72). Figure 3 compares the MB model predictions with experimental volumetric properties of liquid water. The properties of the MB model

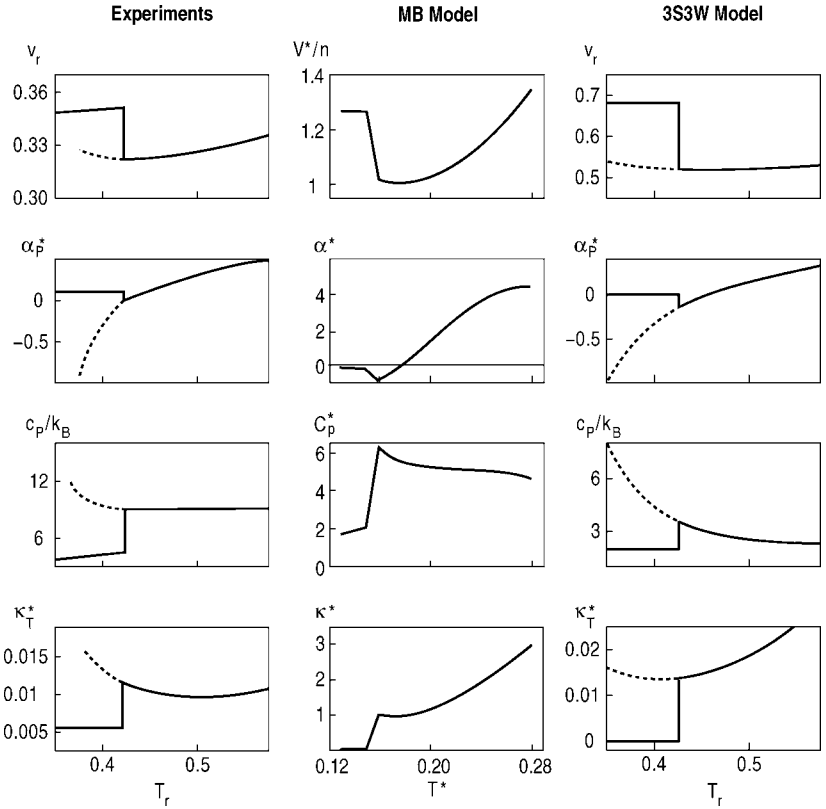

Figure 3 Properties of liquid water: molar volume, thermal expansion coefficient, heat capacity, and isothermal compressibility. *Left*: Experiments (2, 34, 46, 79). *Middle*: MB model water (72). *Right*: 3S3W model water (90). Unbroken lines indicate the stable liquid and crystalline phases; dashed curves represent the supercooled liquid. In reduced variables: $T_r = T/T_C$, $P_r = P/P_C$, $v_r = v/v_C$, $\kappa_T^* = -(\partial \ln v_r/\partial P_r)_{T_r}$, and $\alpha_P^* = (\partial \ln v_r/\partial T_r)_{P_r}$. Subscript C denotes the value at the liquid-vapor critical point.

are given in reduced units—all energies and temperatures are normalized by the energy of an optimal hydrogen bond (e.g., $T^* = k_B T/|\epsilon_{HB}|$, $U^* = U/|\epsilon_{HB}|$). Similarly, all distances are scaled by the length of an idealized hydrogen bond (e.g., $V^* = V/r_{HB}^2$).

Here is the physical basis for these volumetric anomalies in the model. Consider the process of increasing temperature, starting from ice at the melting point ($T_{melt} = 0°C$), through the temperature of maximum density ($T_{md} = 3.984°C$), to the boiling point, $T_{boil} = 100°C$. Upon melting, some of the highly regular ice-like structure is lost because hydrogen bonds are broken. Upon further heating, from T_{melt} to T_{md}, the density increases because hydrogen bond breakage leads to opportunities for van der Waals interactions to pull water molecules closer together. Above T_{md}, up to T_{boil}, further heating weakens all the bonds—van der Waals and hydrogen bonds—leading to lower densities. Hot water acts much like a normal liquid—it expands upon heating—whereas water that is colder than approximately 4°C is anomalous: It becomes denser upon heating. This anomaly is reflected in the thermal expansion coefficient, which is the derivative of volume with temperature. For most liquids, the thermal expansion coefficient is positive. For water, the thermal expansion coefficient changes sign, from negative to positive, at T_{md}.

The model gives a related explanation for the compressibility of water, the change in volume with applied pressure. The compressibility correlates (loosely) with density. At high densities, molecules—of both normal liquids and water—pack together tightly, leading to a lower compressibility, i.e., to less susceptibility to further increases in density with applied pressure. Because there is a maximum in the density of liquid water, this implies that there should be a minimum in the compressibility. For compressibility too, hot water resembles normal liquids, whereas cold water is anomalous.

The heat capacity [$c_P = (\frac{\partial H}{\partial T})_P$] is a measure of a system's ability to absorb thermal energy, for example, through the breaking of bonds. Liquid water's high heat capacity indicates its multiple modes of energy storage, through the breakage of both van der Waals interactions and hydrogen bonds.

THE HYDROPHOBIC EFFECT: THE ANOMALOUS THERMODYNAMICS OF MIXING OIL WITH WATER

Water also has anomalous properties as a solvent. An example is the hydrophobic effect (10, 87) (see Figure 4). The transfer of a nonpolar solute into cold water (approximately room temperature, for example) is opposed by a large entropy, but transfer into hot water (near the boiling point) is opposed instead by a large enthalpy. In simpler solvents, the process of transferring a solute molecule is usually opposed by a relatively small enthalpy at all temperatures. Why is hydrophobic solvation different from simpler solvation?

In the MB model, a nonpolar solute is modeled as a LJ disk with no hydrogen bonding arms (72). Figure 4 compares the free energy, enthalpy, entropy,

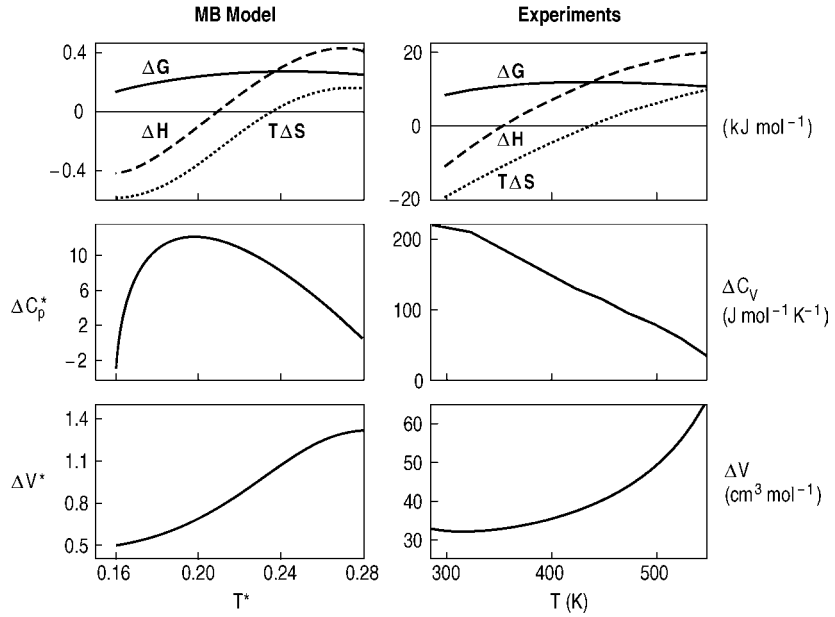

Figure 4 Hydrophobic effect: Transfer thermodynamics of a LJ solute in MB water (*left panels*) versus the experimental transfer of argon from gas into water (*right panels*) (72). See text for reduced units.

heat capacity, and the volume of transfer of an MB nonpolar molecule into water (36, 70–74, 76–78) with experiments (20). The model shows good qualitative agreement with the experiments. Such simulations are much more challenging in detailed three-dimensional models, particularly for properties such as the heat capacity.

The essence of hydrophobicity is the large positive heat capacity of transfer of a nonpolar solute into water. For simpler systems, the heat capacity of transfer is small. What is the origin of this large hydrophobic heat capacity? In 1945, Frank & Evans (30) proposed the iceberg model. According to their model, the first shell of waters around a nonpolar solute is structured, like ice. Heating a solution leads to a melting of this "iceberg," i.e., giving an increased energy and entropy of the first-shell waters, and thus to an increased heat capacity, $C_v = dU/dT$.

Figure 5 shows that the MB model has features of the iceberg model. Figure 6 (see color insert) shows the first-shell water orientational distributions as a function of temperature (72). In cold water, first-shell waters have a slight preference for cage-like structures around nonpolar solutes (hence low entropy, and low energy, reflecting favorable water-water hydrogen bonding). Water molecules avoid pointing hydrogen bonds at the solute to avoid wasting those bonds. In hotter water, the orientational preferences are weaker, hence the structure has melted out.

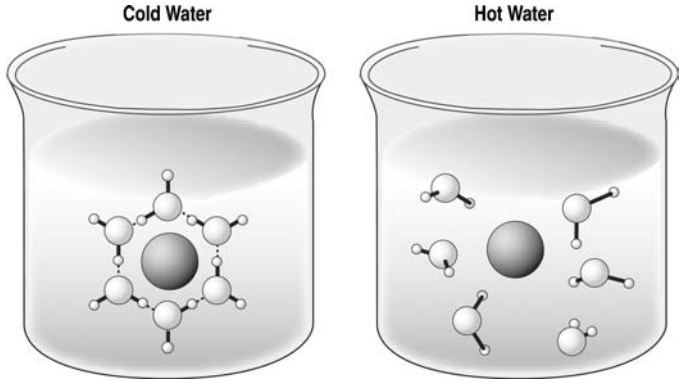

Figure 5 Iceberg model for the large heat capacity of transfer of nonpolar solutes into water.

There are second-shell effects as well, but they are smaller. Historically, the main criticism of the iceberg model has been that first-shell waters cannot be as highly ordered around nonpolar solutes as they can in ice. In the MB model, this ordering is reflected more in the thermodynamics than in the structures. The structural preferences are small, much smaller than in ice.

The Fingerprints of Hydrophobicity Depend on Solute Size

MB model studies of hydrophobicity give an unexpected and interesting result: Transferring a small nonpolar solute (approximately the size of a water molecule) into water shows all the anomalous characteristics of the hydrophobic effect (large positive heat capacity, opposed by entropy at room temperature, opposed by enthalpy at higher temperatures), but transferring a large nonpolar solute (several times the radius of a water molecule) shows no such thermal anomalies. While transferring a large planar nonpolar slab into water would be unfavorable (positive free energy), it would neither be mainly opposed by entropy at room temperature nor have a large heat capacity of transfer, according to MB model simulations. Figure 7 (see color insert) shows the simulations using the MB model for solutes of different sizes (76).

As noted above, for small nonpolar solutes, first-shell waters straddle the solute, losing entropy to gain hydrogen bonding. Increasing the temperature disorders the first-shell waters, breaking hydrogen bonds. However, as the radius of a spherical nonpolar solute grows larger, first-shell waters become increasingly challenged by the geometrical restrictions of the adjacent solute surface, such that they cannot form a full complement of hydrogen bonds with neighboring waters. Hence around solute molecules that are sufficiently large, first-shell water molecules must waste a hydrogen bond, even at room temperature, pointing it directly at the solute surface. The first-shell water wastes this hydrogen bond because it has no geometric alternative. Pointing one hydrogen bond as directly as possible toward the

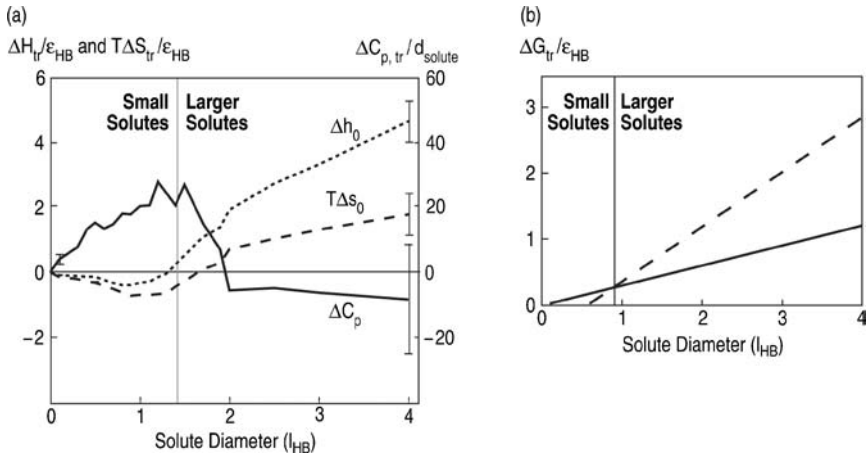

Figure 8 (*a*) MB entropy (*long dash*), enthalpy (*short dash*), and heat capacity (*solid line*) of transferring a nonpolar solute as a function of solute diameter at $T^* = 0.18$ (76). (*b*) MB free energy of transfer as a function of solute diameter at $T^* = 0.18$ (76): extrapolation from small solutes (*solid line*) from large solutes (*dashed line*).

surface gives each water molecule as much conformational freedom as is otherwise possible.

Figure 8*a* shows the thermal consequences. For a small nonpolar solute, the transfer into cold water leads to a large negative entropy (because the first-shell waters become ordered), a large positive heat capacity (because a first-shell structure is formed that melts out with temperature), and a small change in the enthalpy. But for large solutes, the transfer into cold water has rather different physics: the enthalpy is large and positive (because each water breaks a hydrogen bond), the entropy is small (because the surface waters are no more restricted than bulk waters), and the heat capacity is small (because no additional bond breakage or water disordering can be achieved by increasing the temperature). These predictions remain to be tested experimentally. The experimental challenge is that large nonpolar spheres have so little solubility in water that they are detectable only by methods of high sensitivity.

This MB model resolves a puzzle. In discussions among Dill, Hildebrand, Sharp et al., Tanford, and others (24, 37, 38, 68, 86), it was noted that transferring a small nonpolar solute into water costs approximately 25 cal mol$^{-1}A^2$, whereas the interfacial tension between oil and water gives a value approximately threefold larger, 75 cal mol$^{-1}A^2$. The MB model result in Figure 8*b* explains this as the difference between water ordering entropy (around small solutes) and the hydrogen bond breaking enthalpy (around large solutes). Around small solutes the entropic cost of ordering waters is approximately 25 cal mol^{-1}, whereas around large solutes the enthalpic cost of breaking a hydrogen bond is approximately 75 cal mol$^{-1}A^2$ (76).

Solute-Solute Interactions in Water: In Contact or Not?

In 1977, Pratt & Chandler (62) addressed whether two nonpolar solutes in water come into contact with each other or are stable when separated by a single layer of water. The first situation is called the contact minimum, and the second is called the solvent-separated minimum. We have explored this question using the MB model. Figure 9*a* (see color insert) shows the result: When two nonpolar solutes are small, they prefer the solvent-separated state, but when two solutes are large, they come into contact.

The reason is shown in Figure 9*b*. A small solute is surrounded by a water clathrate cage. When two small solute molecules come together, their clathrate cages share a common interface, i.e., a sort of fence of water separates the solutes. In contrast, larger solutes cannot form a stable clathrate interface with a good hydrogen-bonded structure. Hence, large solutes come into contact to minimize the surface area of solute exposure to water. For small solutes, the tendency to minimize the free energy is not equivalent to a tendency to minimize their shared contact area because other aspects of local geometry become more important on that size scale than just the surface area.

KOSMOTROPES ARE IONS THAT ORDER WATER; CHAOTROPES ARE IONS THAT DISORDER WATER

How do ions dissolve in water? Since the 1930s, an important unifying concept has been the idea that some ions are kosmotropes (from kosmos, meaning orderly) and some are chaotropes (from chaos, meaning disorder). Kosmotropic ions order water and chaotropic ions disorder water, according to various experimental measures. For example, the change of entropy of hydration water owing to the presence of an ion can be either positive or negative (47) (see Figure 10). The dissolution of small ions, such as lithium, in water leads to a large negative entropy change, indicating that lithium orders water. Lithium is a kosmotrope. In contrast, dissolving cesium in water leads to a positive entropy change. Cesium is a chaotrope (41).

Another measure of the ionic ordering and disordering of water is given by the viscosity of water $\eta(c)$ as a function of the ion concentration c. The Jones-Dole B coefficient is a measure of the ion-water interaction (64):

$$\eta(c)/\eta_0 = 1 + Ac^{1/2} + Bc + \ldots, \qquad 2.$$

where η_0 is the viscosity of pure water and A is a concentration-independent coefficient that describes Debye-Huckel-like counterion screening effects at low ion concentrations. The B coefficient describes the effect of higher ion concentrations; B is positive for lithium ions and negative for cesium ions, for example, indicating that lithium increases water's viscosity and cesium decreases water's viscosity. Hence, viscosity enhancement is regarded as another measure of ordering. Another experimental property that is used to characterize the ionic ordering of water is the

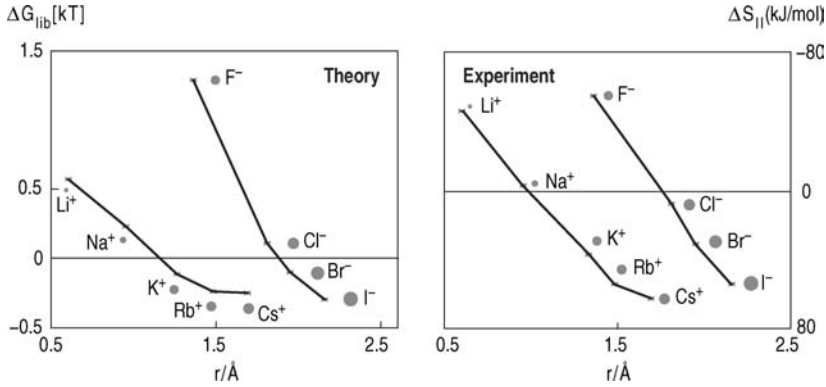

Figure 10 (*a*) MB + dipole model liberation free energy, ΔG_{lib}, at $T^* = 0.20$ (41). (*b*) The change of entropy, ΔS_{II}, of water brought about by the presence of an ion (47) at 198 K for different ions.

activation energy, ΔE_i, needed to strip a water molecule away from an ion relative to the activation energy needed to strip a water molecule away from another water molecule (66). Kosmotropic ions are strongly bound to their neighboring water molecules and therefore have a large positive activation energy; this is not the case for chaotropes. Strong correlations between water solvation entropies and viscosity enhancements indicate that an ion's designation as a chaotrope or kosmotrope is general and not restricted to a single experimental observable (47).

Figure 10 shows two prominent aspects of ion solvation in water. First, water ordering depends systematically on the ionic radius. Water is ordered by smaller ions and disordered by larger ions. Second, there is an offset between anions and cations. F^- has about the same radius as K^+, yet the negative ion acts as if it were smaller in causing greater water ordering. What is the explanation for these two effects?

Figure 11*a* (see color insert) shows the model we use to study ion solvation: The MB + dipole model includes a dipole moment on each water molecule in addition to the MB model interactions described above. The dipole is negative at the center of the water disk and positive at a point approximately 60% of the way along one of the hydrogen bonding arms (41). This is intended to mimic the dipole moment of water, which has a partial negative charge on the oxygen at the center and a partial positive charge on each hydrogen atom. Using this model, we compute the liberation free energies of water next to an ion, ΔG_{lib}, as suggested by Chong & Hirata (17). The results are in good agreement with the experimental results of Samoilov (66).

The model explains the ionic ordering of water in terms of the charge density on the ion. The positive end of water's dipole tends to point toward a negative ion, or away from a positive ion. The electrostatic interaction with water is strongest for a small ion because it can reach closest to water's dipole, and weakest for a

large ion (see Figure 11*b*). In short, small ions such as lithium get closer to waters and order them more strongly than larger ions such as cesium.

Figure 11*c* also explains the charge asymmetry. An anion can come closer to the positive end of water's dipole (which is near the surface of the water molecule) than a cation can come to the negative end of water's dipole (which is at the center of the water). Hence, for a given ionic radius, a negative ion interacts more strongly with water than a positive ion does.

Figure 12 (see color insert) illustrates these points differently. Around a small ion such as lithium, waters are ordered predominantly by the electrostatic interactions of their dipoles with the ion. However, around a large ion such as cesium, electrostatic interactions are weaker, so water ordering is dominated by water-water hydrogen bonding. In that regard, large ions act much like nonpolar solutes.

THE HOFMEISTER SERIES IS A RANK-ORDERING OF SALT EFFECTS ON HYDROPHOBIC INTERACTIONS

Proteins precipitate out of solution (i.e., are salted out) if they are put into salty water containing certain types of ions, yet proteins become more soluble (salted in) in water containing other types of ions. Ions can be rank-ordered by the extent to which they solubilize or precipitate proteins. This rank-ordering is called the Hofmeister series, after F. Hofmeister, who made the first observation of this effect more than a century ago (39). These effects are observed at high concentrations of salts, typically greater than 0.1 M, and are thus not predominantly due to long-range electrostatics, which are largely shielded in solutions of high salt concentrations. Experiments show that adding salt to water reduces the solubility of a nonpolar solute in water in roughly the same rank-ordering and at the same concentrations as those found for protein precipitations (14, 19). The general interpretation is that Hofmeister effects are ionic effects on hydrophobic interactions through first- and second-neighbor water shells (52).

The degree to which a salt reduces, for example, benzene's solubility in water depends on the type of salt (52) (Figure 13, see color insert). The molar solubility, c, of a nonpolar solute in salt water is typically given by the Setchenow equation (4):

$$\ln[c/c(0)] = -k_s c_s, \qquad 3.$$

where $c(0)$ is the molar solubility in pure water, c_s is the molar concentration of the salt, and k_s is the salt's Setchenow salting-out coefficient.

What explains the Hofmeister effect? We compared experimental Setchenow coefficients with the computed free energy of transferring a hydrophobic solute into MB + dipole water with salt (41). We found good qualitative agreement between the model and the experiments. The results support a volume-exclusion mechanism (see Figure 13*a*). As noted above, a large ion, such as cesium, acts much like a hydrophobic solute. The benzene sees the large ion as largely another

hydrophobic molecule and readily comes into contact with it. In contrast, benzene cannot penetrate the first shell of waters around a small ion such as lithium because lithium binds those waters tightly through electrostatic forces on the water's dipole. Hence, benzene has less volume accessible to it in a solution with lithium than in a solution with cesium at the same ion concentration (41).

TOWARD ANALYTICAL MODELS OF WATER

Even with modern computer simulations of water, it is of considerable value to develop theories that are analytical because they can give complementary insights, they do not require extensive computational resources, they can explore a wider range of variables and parameters, they can suggest mathematical functional forms that can be used for engineering, and they can lead to better and more computationally efficient models of solvation.

The simplest model of liquids is the van der Waals equation of state. The van der Waals model treats the steric repulsions and the centrosymmetric attractions between molecules; it explains the sharp boiling transition and the critical point. But by itself, the van der Waals model cannot describe water because it does not deal with the strong orientational attractions due to water's hydrogen bonding, and it therefore does not predict water's interesting anomalies. Hydrogen bonding is central to water's peculiar behavior (1, 5, 22, 54).

Recent analytical treatments of water (3, 60, 88, 89) have extended the van der Waals model to incorporate hydrogen bonding interactions. These approaches introduce effective intermolecular potentials that account approximately for water's open (low-density) and bonded (low-energy, low-entropy) states (7, 15, 27, 28, 35, 56, 58, 59, 69). Such models predict many of liquid water's distinctive thermodynamic properties, but they do not directly relate water's hydrogen bonding structures to its thermodynamic properties. Thus, they cannot give insights into the ordered phases of water (e.g., ice) or water structuring around solutes. Here, we describe two analytical treatments that predict the properties of water from its hydrogen bonding energetics and structure.

A Three-State Three-Water Mean-Field Model

Here we review a simple three-state three-water (3S3W) model (90–92). Each water molecule is a two-dimensional disk with diameter d having three identical bonding arms arranged as shown in the MB model. Although this two-dimensional geometry is similar to that of the MB model, the energetics is slightly different so that the model can be treated analytically. There are three different ensembles of local states of three neighboring water molecules with different local structures, volumes, and energy levels. The states are shown in Figure 14 (see color insert): one is a hydrogen-bonded ice-like or cage-like state of three neighboring water molecules having a relatively open structure; one is a van der Waals–bonded state

of three molecules having a higher density; and one is an expanded state, whereby the three waters do not interact with each other.

State 1: Cage-like The state of lowest energy is a cooperative hydrogen-bonded configuration similar to the cage-like structures found in ice (72). In this state, the hydrogen bond B—C is made. The energy, u_1, depends on the angle of hydrogen bond B—C with hydrogen bond A—B, $u_1(\phi) = -\epsilon_{HB} + k_S\theta^2$, where k_S is the angular spring constant and θ is the angle shown in Figure 14. The B—C hydrogen bond is cooperative insofar as its strength is modulated by the angle with A—B. ϵ_{HB} is the energy associated with a perfect B—C hydrogen bond, i.e., one in which the angle between B—C and A—B is 120 degrees. The local two-dimensional volume of the perfectly bonded cage-like state is $v_1 = 3\sqrt{3}d^2/4$.

State 2: Dense The next higher energy level is a dense state, in which molecules A, B, and C are in van der Waals contact, but there is no B—C hydrogen bond. The energy of this state is $u_2 = -\epsilon_d$, where ϵ_d is a constant, and the local volume is given by $v_2 = (2 + \sqrt{3})d^2/4$.

State 3: Expanded The highest energy level is an expanded state that has neither hydrogen bonds nor van der Waals contacts. Its energy is $u_3 = 0$, and its local volume is assumed to be that of an excluded-volume gas $v_3 = (\beta P)^{-1} + v_2$, where $\beta = (k_B T)^{-1}$, k_B is Boltzmann's constant, T is temperature, and P is pressure. Interactions beyond the triplet level are accounted for in a self-consistent way by incorporating a background cohesive energy—Na/v, where a is the van der Waals dispersion parameter and v is the average molar volume (90).

The isothermal-isobaric partition function, $\Delta_B(T, P, N)$, for each molecule B can be expressed as an integral over the allowed positions and orientations for each state type and summed over the three types of states—cage-like, dense, and expanded (90). The partition function for the entire system of N molecules $\Delta = (\Delta_{\text{cell}})^N/N!$ is given by

$$\Delta = \left(\sum_{j=1}^{3} \Delta_j\right)^N. \qquad 4.$$

Here $\Delta_j = g_j \exp[-\beta(\langle u_j\rangle + P v_j)]$, where $\langle u_j\rangle$ is the ensemble-averaged energy of state j,

$$\langle u_1\rangle = -\epsilon_{HB} + \frac{1}{2\beta} - \sqrt{\frac{k_S\pi}{\beta}}\frac{\exp(-\beta k_S\pi^2/9)}{3\text{erf}\left(\sqrt{\beta k_S\pi^2/9}\right)} \qquad 5.$$

$$\langle u_2\rangle = -\epsilon_d$$

$$\langle u_3\rangle = 0$$

and the g_j's are the corresponding densities of states:

$$g_1 = 2\pi d^2 c(\beta) e \frac{\mathrm{erf}\left(\sqrt{\beta k_S \pi^2/9}\right)}{\sqrt{\beta k_S \pi}} \exp\left(\frac{1}{2} - \frac{\sqrt{\beta k_S \pi}\exp(-\beta k_S \pi^2/9)}{3\mathrm{erf}\left(\sqrt{\beta k_S \pi^2/9}\right)}\right) \quad 6.$$

$$g_2 = 2\pi d^2 c(\beta) e$$

$$g_3 = 2\pi c(\beta) e \frac{1}{\beta P}.$$

To predict experimental observables, the chemical potential is given by $\mu(\beta, P) = -(\beta N)^{-1} \ln \Delta$, and the molar volume (i.e., the equation of state) is given by $v(\beta, P) = (\partial \mu / \partial P)_\beta$ (90), for example.

THE THREE-STATE THREE-WATER MODEL PREDICTS WATER'S ANOMALOUS PROPERTIES FROM HYDROGEN-BONDING STRUCTURE AND GEOMETRY This 3S3W model is simple enough that properties can be calculated in a few seconds on a personal computer. Figure 3 shows that the model (90, 91) predicts liquid water's expansion upon cooling and its minima in volume, isothermal compressibility, and heat capacity (2, 34, 46, 79).

The model also predicts the populations f_j of the three types of local states ($j = 1, 2, 3$) as a function of temperature and pressure (see Figure 15). Cold liquid water molecules are predominantly in cage-like configurations with open structures. As the temperature is raised, hydrogen bonds break, and the cages collapse into denser states of higher enthalpy. This explains cold water's negative thermal expansion coefficient and its unusually large heat capacity. Further heating breaks the van der Waals contacts, leading to hot water's expansion with temperature. Liquid water shifts with temperature from cage-like to dense to expanded configurations, accounting for the density reversals.

What are the effects of pressure? Applying pressure to the cold liquid collapses the open cage-like states into dense structures (90), readily explaining cold water's large isothermal compressibility in terms of Le Chatelier's principle: Compression shifts the liquid structure away from the high-volume cages to the low-volume dense structures. In addition, the model correctly predicts that the anomalies shown in Figure 3 are suppressed at high pressures (90) because the high-pressure van der Waals state of water more nearly resembles a normal liquid than the low-pressure cage-like state does. Thus, applying pressure to cold water converts it to a more normal liquid.

Figure 15 also shows good qualitative correspondence between the three predicted states of the model water with experimental populations observed in IR spectra (50). On the basis of an analysis of OH stretching bands, Luck (50) has identified three distinct OH states present in water (in order of increasing energy): strongly cooperative hydrogen bonded, weakly cooperative hydrogen bonded, and nonbonded. Figure 15 shows that these observed populations correlate well with the cage-like, dense, and expanded states, respectively, of the 3S3W model.

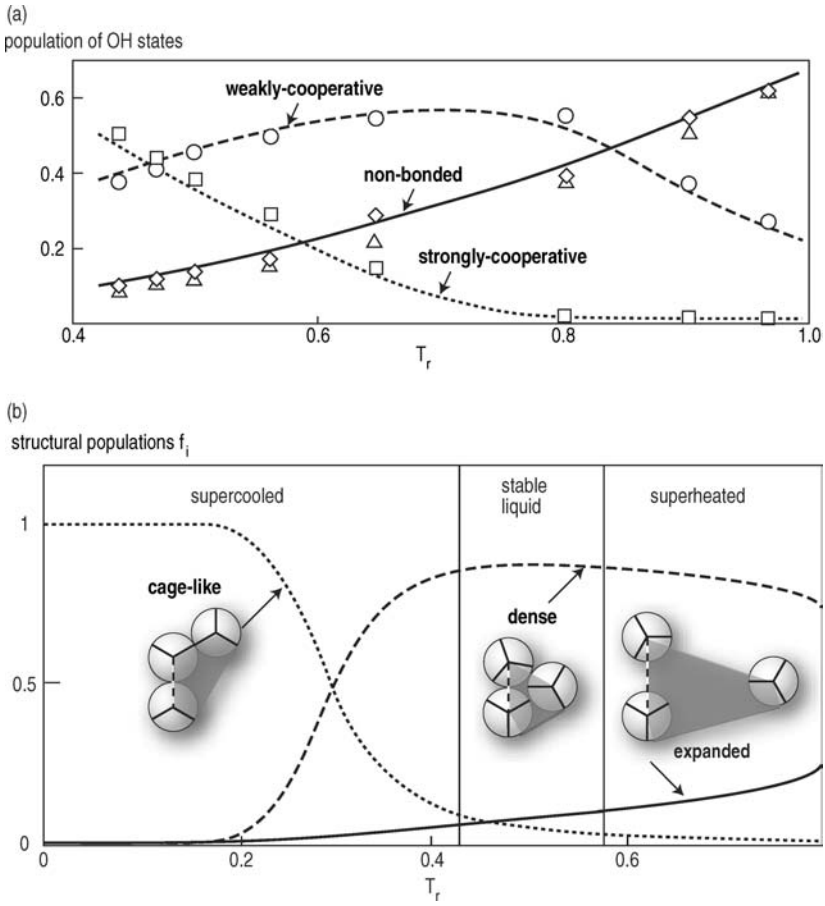

Figure 15 (*a*) Populations of OH states versus temperature T_r along water's saturation curve as determined from IR spectra [adapted from figure 5 of (50)]. (*b*) Populations, f_j, of the three states—cage-like, dense, and expanded—versus temperature T_r for the 3S3W model liquid at atmospheric pressure (91). The vertical lines indicate the freezing and boiling points (see Figure 16).

THE THREE-STATE THREE-WATER MODEL PREDICTS THE PHASE DIAGRAM OF WATER

The 3S3W model predicts a freezing transition. We considered two crystalline forms of water: low-pressure (LP) and high-pressure (HP) ice. LP ice is an open cage-like MB solid found at low pressures and temperatures (72). HP ice is the same as LP ice, except that HP ice has an additional water molecule in the center of each cage (see Figure 16); it is a self-clathrate (57).

Figure 16 compares the model predictions with the experimental phase diagram for water. The model correctly predicts a vapor-liquid transition that terminates at

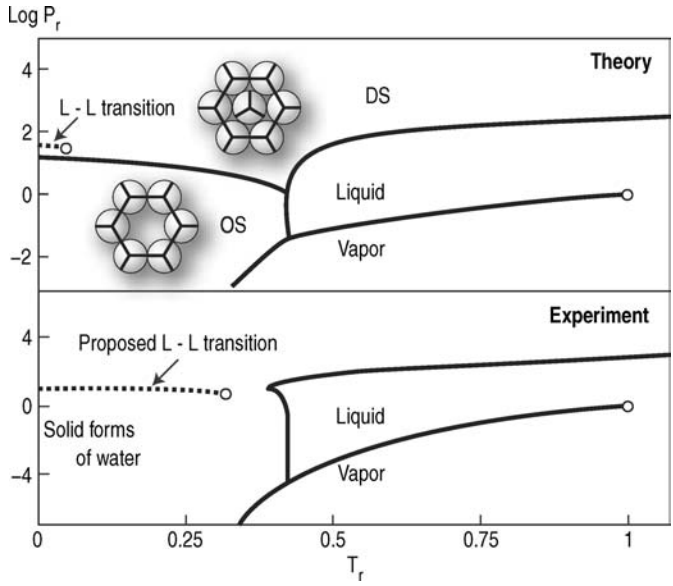

Figure 16 Phase diagram of the 3S3W model (*top*) compared with experiments (*bottom*): pressure P_r versus temperature T_r (91). Dashed curves locate the metastable liquid-liquid (L-L) transition in the theory and a schematic of its proposed location in water (see 54). LP ice consists of open cages in which each molecule bonds to three neighbors. HP ice is LP ice, except with an additional molecule in the center of each cage.

a critical point, and it predicts freezing transitions to the LP and HP forms of ice at low and high pressure, respectively. LP ice correctly shows a negatively sloped melting curve (contraction upon melting), whereas HP ice displays the normal positively sloped melting curve (expansion upon melting). The two ice forms are separated by a first-order phase transition. The melting and boiling curves converge to a triple point, below which only the vapor or solid states are thermodynamically stable.

The 3S3W model also predicts glassy behavior in supercooled water. Recent experiments show that glassy water (i.e., amorphous ice) has an apparent first-order transition between its low-density and high-density forms at low temperature and high pressure (53, 54). This observation suggests the insightful hypothesis (59) [although not yet experimentally verified (22, 54)] that the transformation may reflect an underlying liquid-liquid phase transition in supercooled water. Consistent with this hypothesis, the 3S3W model predicts a low-temperature transition between two supercooled liquid phases: a predominantly cage-like phase at low temperatures that melts out to a denser state of water at higher temperatures.

Treating Mercedes-Benz Water Using Thermodynamic Perturbation and Integral Equation Theories

Another analytical strategy is based on thermodynamic perturbation and integral equation methods. This strategy may be particularly useful for solutes that are not at high dilution in water, for example, in multicomponent solutions. Wertheim recently developed a theory for fluids of molecules that interact with highly directional attractive forces (45, 96, 97).

We have applied a thermodynamic perturbation theory (TPT) and an integral equation theory (IE) to the MB model. The key quantity in the TPT approach (96) is the Helmholtz free energy A of a system,

$$A = A_{LJ} + A_{HB}, \qquad 7.$$

where A_{LJ} is the Helmholtz free energy of a LJ system and A_{HB} is the hydrogen bond contribution. The term A_{LJ} is calculated using the Barker-Henderson perturbation theory (33), with hard disks as a reference system. The three hydrogen bonds of the MB molecule (see Figure 1) are equivalent, so the number of distinguishable states is four: Each water molecule has from zero to three hydrogen bonds. For the hydrogen bond contribution to the Helmholtz free energy, we use the expression (94)

$$\frac{A_{HB}}{Nk_BT} = 3\left(\log x_i - \frac{x_i}{2} + \frac{1}{2}\right), \qquad 8.$$

where N is the number of particles and x_i is the fraction of molecules not bonded at arm i, which is obtained from a mass-action equation of the form

$$x_i = \frac{1}{1 + 3\varrho x_i \Delta}, \qquad 9.$$

where ϱ is the total number density and Δ is defined by

$$\Delta = 2\pi \int g_{LJ}(r)\bar{f}_{HB}(r) r dr, \qquad 10.$$

where $\bar{f}_{HB}(r)$ is an orientationally averaged Mayer function for the hydrogen-bonding potential of one site. The pair distribution function $g_{LJ}(r)$ is obtained by solving the Percus-Yevick equation for the LJ disks (33). Details are given in Reference 94.

INTEGRAL EQUATION APPROACH The IE theory is based on the multidensity version of the Ornstein-Zernike integral equation (94–96). IE goes beyond TPT in giving spatial distributions in addition to thermodynamic properties. The basic equation of this approach is the associative Ornstein-Zernike equation,

$$\hat{\mathbf{h}}(k) = \hat{\mathbf{c}}(k) + \hat{\mathbf{c}}(k)\boldsymbol{\rho}\hat{\mathbf{h}}(k), \qquad 11.$$

where $\hat{\mathbf{h}}(k)$ and $\hat{\mathbf{c}}(k)$ are the matrices, the elements are the Fourier transforms of the partial correlation functions $h_{ij}(r)$ and $c_{ij}(r)$, respectively. $\boldsymbol{\rho}$ is the matrix containing number densities (94). We use the Polymer Percus-Yevick (PPY) closure (96).

The main approximation of the TPT and IE theories described above is the use of orientationally averaged functions to take advantage of the simplicity of centrosymmetric interactions. According to that approximation, the hydrogen bonding arms are not at fixed angles of 120 degrees with respect to each other, but rather are approximated as being randomly oriented with respect to each other.

These methods predict well the high-temperature properties (above $T^* = 0.24$) of both pure MB water and MB nonpolar solutes in water. The IE and TPT treatments, however, deviate from the MB model Monte Carlo simulations for cold liquid water ($T^* = 0.18$) because of limitations of the random-angle approximation (95). A key property of MB water, and of real water, is that the hydrogen bonding vectors within each molecule have fixed relative orientations.

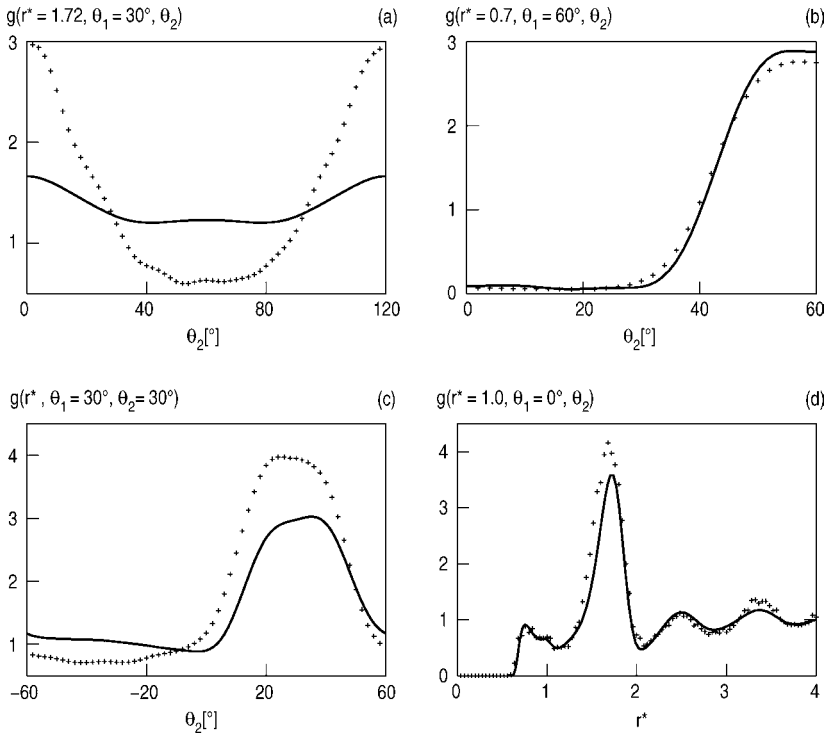

Figure 17 Two-dimensional slices of $g(r^*, \theta_1, \theta_2)$ as a function of θ_2 with (*a*) r^* and θ_1 fixed at 0.7 and 60°, (*b*) $r^* = 1.0$ and $\theta_1 = 0°$, (*c*) $r^* = 1.72, \theta_1 = 30°$, and (*d*) as function of r^* with $\theta_1 = \theta_2 = 30°$. The MC results (*symbols*), PMSA lines; $T^* = 0.20$ and $\rho^* = 0.90$.

ORIENTATION-DEPENDENT INTEGRAL EQUATION THEORY To improve upon the TPT and IE methods, we have generalized the Ornstein-Zernike equation to treat angular correlations (93). We expanded the two-particle correlation function in a complete set of orthogonal angular functions. We studied two different approximate closure conditions, PPY and the Polymer MSA (PMSA) closure, and found the latter to be slightly better.

Solving the orientation-dependent integral equation theory (ODIET) yields an angle-dependent two-particle distribution function, $g(r^*, \theta_1, \theta_2)$. Including the explicit dependence on the intramolecular hydrogen bond angle improves the prediction of structure, relative to the angle-averaged models above, particularly of the second and third solvation shells.

Figure 17 shows predicted angular distributions, two-dimensional slices of $g(r, \theta_1, \theta_2)$ as a function of θ_2, for $T^* = 0.20$ and $\rho^* = 0.90$. The ODIET approach captures the qualitative features of the orientation dependence of water-water interactions.

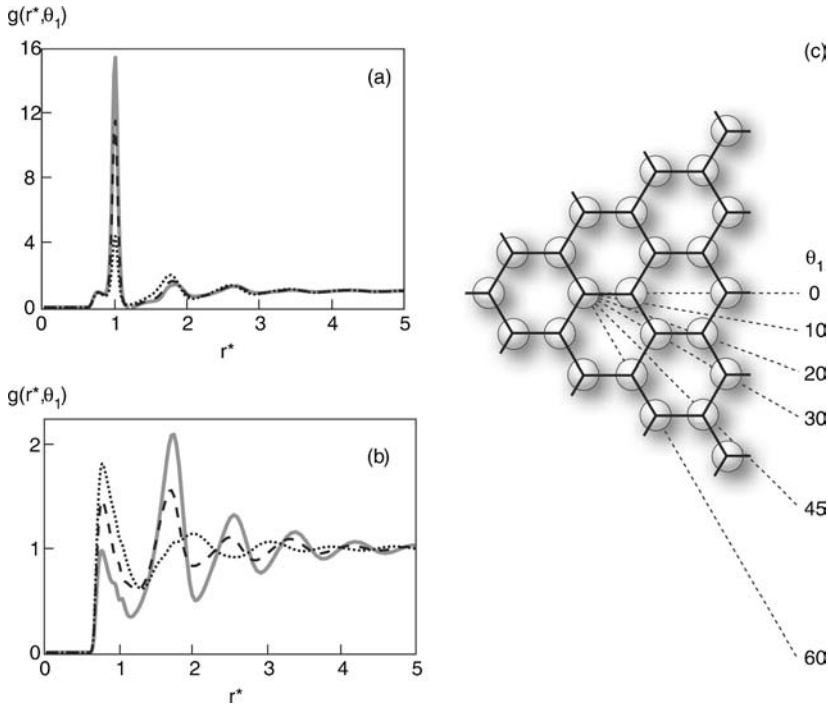

Figure 18 Orientational pair distribution, $g(r, \theta_1)$, for various orientations θ_1 of the first molecule, averaged over all possible θ_2 values, together with a picture showing the arrangement of molecules in the solid phase, i.e., for the MB model ice. (*a*) $\theta_1 = 0^\circ$ (*full line*), $\theta_1 = 10^\circ$ (*dashed line*), and $\theta_1 = 20^\circ$ (*dotted line*). (*b*) $\theta_1 = 30^\circ$ (*full line*), $\theta_1 = 45^\circ$ (*dashed line*), and $\theta_1 = 60^\circ$ (*dotted line*). (*c*) Arrangement of MB molecules in the solid phase.

Figure 18 (93) shows the degree of MB ice-like ordering in the liquid. The first molecule is fixed in orientation θ_1, and we calculate the distributions with respect to r^*, averaging over all θ_2 values [$g(r^*, \theta_1) = \langle g(r^*, \theta_1, \theta_2)\rangle_{\theta_2}$].

In short, simple pair correlation functions, $g(r)$, are too averaged to contain much information about water structure and cages. The orientational distribution functions $g(r, \theta_1, \theta_2)$ contain much more information about water structure. The ODIET method gives much better predictions than simpler integral equation methods, although still not perfect, for these angle-dependent properties of water.

SUMMARY

We have reviewed simplified models and the insights they give into water, including its thermal properties, phase diagram, volumetric anomalies, and its properties as a solvent for nonpolar solutes and ions. Monte Carlo simulations of MB water have provided a springboard for new analytical treatments, such as a 3S3W mean-field model and thermodynamic perturbation and IE methods, that can be used for orientational liquids such as water. These models suggest that many of the qualitative and global properties of water—water's thermodynamics, its volume anomalies, and its properties in the hydrophobic effect and as a solvent for ions—may not depend strongly on atomic details or on water's tetrahedrality per se; rather, they depend on water's fixed angular interactions owing to its hydrogen bonding geometry. One long-term goal of simplified modeling is to develop more computationally efficient ways to understand pure water and aqueous solvation.

The *Annual Review of Biophysics and Biomolecular Structure* is online at http://biophys.annualreviews.org

LITERATURE CITED

1. Angell CA. 1983. Supercooled water. *Annu. Rev. Phys. Chem.* 34:593–630
2. Angell CA, Oguni M, Sichina WJ. 1982. Heat capacities of water at extremes of supercooling and superheating. *J. Phys. Chem.* 86:998–1002
3. Ashbaugh HS, Truskett TM, Debenedetti PG. 2002. A simple molecular thermodynamic theory of hydrophobic hydration. *J. Chem. Phys.* 116:2907–21
4. Baldwin RL. 1996. How Hofmeister ion interactions affect protein stability. *Biophys. J.* 71:2056–63
5. Ball P. 1999. *Life's Matrix: A Biography of Water*. New York: Farrar, Straus, & Giroux
6. Barker JA, Watts RO. 1969. Structure of water: a Monte Carlo calculation. *Chem. Phys. Lett.* 3:144–45
7. Bellissent-Funel MC. 1998. Is there a liquid liquid phase transition in supercooled water? *Europhys. Lett.* 42:161–66
8. Ben-Naim A. 1971. Statistical mechanics of "waterlike" particles in two dimensions. I. Physical model and application of the Percus-Yevick equation. *J. Chem. Phys.* 54:3682–95
9. Ben-Naim A. 1974. *Water and Aqueous Solutions*. New York: Plenum. 474 pp.
10. Ben-Naim A. 1983. *Hydrophobic Interactions*. New York: Plenum. 311 pp.
11. Berendsen HJC, Grigera JR, Straatsma TP. 1987. The missing term in the effective

pair potentials. *J. Phys. Chem.* 91:6269–71
12. Bernal JD, Fowler RH. 1933. A theory of water and ionic solutions, with particular reference to hydrogen and hydroxyl ions. *J. Chem. Phys.* 1:515–48
13. Bol W. 1982. Monte-Carlo simulations of fluid systems of waterlike molecules. *J. Mol. Phys.* 45:605–16
14. Cacace MG, Landau EM, Ramsden JJ. 1997. The Hofmeister series: salt and solvent effects on interfacial phenomena. *Q. Rev. Biophys.* 30:241–77
15. Canpolat M, Starr MR, Sadr-Lahijany A, Scala O, Mishima S, et al. 1998. Local structural heterogeneities in liquid water under pressure. *Chem. Phys. Lett.* 294:9–12
16. Carravetta V, Clementi E. 1984. Water-water interaction potential: an approximation of the electron correlation contribution by a functional of the SCF density matrix. *J. Chem. Phys.* 81:2646–51
17. Chong SH, Hirata F. 1997. Ion hydration: thermodynamic and structural analysis with an integral equation theory of liquids. *J. Phys. Chem. B* 101:3209–20
18. Clementi E, Habitz P. 1983. A new two-body water-water potential. *J. Phys. Chem.* 87:2815–20
19. Collins KD, Washabaugh MW. 1985. The Hofmeister effect and the behaviour of water at interfaces. *Q. Rev. Biophys.* 18:323–422
20. Crovetto R, Fernandez-Prini R, Japas ML. 1982. Contribution of the cavity-formation or the hard-sphere term to the solubility of simple gases in water. *J. Phys. Chem.* 86:4094–95
21. Dahl LW, Andersen HC. 1983. Cluster expansions for hydrogen-bonded fluids. III. Water. *J. Chem. Phys.* 78:1962–79
22. Debenedetti PG. 1996. *Metastable Liquids*. Princeton, NJ: Princeton Univ. Press. 411 pp.
23. Debenedetti PG. 2003. Supercooled and glassy water. *J. Phys. Condens. Matter* 15:R1669–726
24. Dill KA. 1990. The meaning of hydrophobicity. *Science* 250:297–98
25. Dill KA. Brombert S, eds. 2003. *Molecular Driving Forces*, pp. 571. New York: Garland Sci.
26. Eisenberg D, Kauzmann W. 1969. *The Structure and Properties of Water*. Oxford, UK: Oxford Univ. Press
27. Errington JR, Debenedetti PG, Torquato S. 2001. Relationship between structural order and the anomalies of liquid water. *Nature* 409:318–21
28. Errington JR, Debenedetti PG, Torquato S. 2002. Cooperative origin of low-density domains in liquid water. *Phys. Rev. Lett.* 89:215503
29. Ferguson DM. 1995. Parameterisation and evolution of a flexible water model. *J. Comput. Chem.* 16:501–11
30. Frank HS, Evans MW. 1945. Free volume and entropy in condensed systems. III. Entropy in binary liquid mixtures; partial molal entropy in dilute solutions; structure and thermodynamics in aqueous electrolytes. *J. Chem. Phys.* 13:507–32
31. Franks F, ed. 1972–1982. *Water: A Comprehensive Treatise*, Vols. 1–7. New York: Plenum
32. Guillot B. 2002. A reappraisal of what we have learnt during three decades of computer simulations on water. *J. Mol. Liq.* 101:219–60
33. Hansen JP, McDonald IR. 1986. *Theory of Simple Liquids*. London: Academic
34. Hare DE, Sorensen CM. 1986. Densities of supercooled H_2O and D_2O in 25 μm glass capillaries. *J. Chem. Phys.* 84:5085–89
35. Harrington S, Zhang R, Poole PH, Sciortino F, Stanley HE. 1997. Liquid-liquid phase transition: evidence from simulations. *Phys. Rev. Lett.* 78:2409–12
36. Haymet ADJ, Silverstein KAT, Dill KA. 1996. Hydrophobicity reinterpreted as 'minimisation of the entropy penalty of solvation.' *Faraday Discuss.* 103:117–24
37. Hildebrand JH. 1968. A criticism of the term "hydrophobic bond". *J. Phys. Chem.* 72:1841–42

38. Hildebrand JH. 1979. Is there a "hydrophobic effect"? *Proc. Natl. Acad. Sci. USA* 76:194
39. Hofmeister F. 1888. Zur Lehre von der Wirkung der Salze. *Arch. Exp. Pathol. Pharmakol.* 24:247–60
40. Horne RA, ed. 1972. *Water and Aqueous Solutions: Structure, Thermodynamics, and Transport Properties*. New York: Wiley-Intersci. 837 pp.
41. Hribar B, Southall NT, Vlachy V, Dill KA. 2002. How ions affect the structure of water. *J. Am. Chem. Soc.* 124:12302–11
42. Hummer G, Garde S, Garcia AE, Pratt LR. 2000. New perspectives on hydrophobic effects. *Chem. Phys.* 258:349–70
43. Jorgensen WL. 1981. Transferable intermolecular potential functions for water, alcohols, and ethers. Application to liquid water. *J. Am. Chem. Soc.* 103:335–40
44. Jorgensen WL, Chandrasekhar J, Madura JD, Impey RW, Klein ML. 1983. Comparison of simple potential functions for simulating liquid water. *J. Chem. Phys.* 79:926–35
45. Kalyuzhnyi YV, Holovko MF, Haymet ADJ. 1991. Integral equation theory for associating fluids: weakly associating 2-2 electrolytes. *J. Chem. Phys.* 95:9151–64
46. Kell GS. 1967. Precise representation of volume properties of water at one atmosphere. *J. Chem. Eng. Data* 12:66–69
47. Krestov GA. 1991. *Thermodynamics of Solvation*. New York: Horwood. 284 pp.
48. Lie GC, Clementi E. 1975. Study of the structure of molecular complexes. XII. Structure of liquid water obtained by Monte Carlo simulation with the Hartree-Fock potential corrected by inclusion of dispersion forces. *J. Chem. Phys.* 62:2195–99
49. Lie GC, Clementi E, Yoishimine M. 1976. Study of the structure of molecular complexes. XIII. Monte Carlo simulation of liquid water with a configuration pair potential. *J. Chem. Phys.* 64:2314–23
50. Luck WAP. 1998. The importance of cooperativity for the properties of liquid water. *J. Mol. Struct.* 448:131–42
51. Matsuoka O, Clementi E, Yoishimine M. 1976. CI study of the water dimer potential surface. *J. Chem. Phys.* 64:1351–61
52. McDevit WF, Long FA. 1952. The activity coefficient of benzene in aqueous salt solutions. *J. Am. Chem. Soc.* 74:1773–81
53. Mishima O, Calvert LD, Whalley E. 1985. An apparently first-order transition between two amorphous phases of ice induced by pressure. *Nature* 314:76–78
54. Mishima O, Stanley HE. 1998. The relationship between liquid, supercooled, and glassy water. *Nature* 396:329–35
55. Nezbeda I. 1997. Simple short-ranged models of water and their application. A review. *J. Mol. Liq.* 73–74:317–36
56. Paschek D, Geiger A. 1999. Simulation study on the diffusive motion in deeply supercooled water. *J. Phys. Chem. B* 103: 4139–46
57. Pauling L. 1939. *The Nature of the Chemical Bond*. London: Oxford Univ. Press
58. Poole PH, Essman U, Sciortino F, Stanley HE. 1993. Phase diagram for amorphous solid water. *Phys. Rev. E* 48:4605–10
59. Poole PH, Sciortino F, Essman U, Stanley HE. 1992. Phase behavior of metastable water. *Nature* 360:324–28
60. Poole PH, Sciortino F, Grande T, Stanley HE, Angell CA. 1994. Effect of hydrogen bonds on the thermodynamic behavior of liquid water. *Phys. Rev. Lett.* 73:1632–35
61. Pople JA. 1951. Molecual association in liquids. II. Theory of the structure of water. *Proc. R. Soc. London Ser. A* 205:163–78
62. Pratt LR, Chandler DJ. 1977. Theory of the hydrophobic effect. *J. Chem. Phys.* 67:3683–704
63. Robinson GW, Zhu SB, Singh S, Evans M. 1996. *Water in Biology, Chemistry and Physics: Experimental Overviews and Computational Methodologies*. Singapore: World Sci.
64. Robinson RA, Stokes RH. 2002. *Electrolyte Solutions*. New York: Dover. 571 pp.
65. Rowlinson JS. 1951. The lattice energy of ice and the second virial coefficient of water vapour. *Trans. Faraday Soc.* 47:120–29

66. Samoilov OY. 1957. A new approach to the study of hydration of ions in aqueous solutions. *Discuss. Faraday Soc.* 24:141–46
67. Samoilov OY. 1957. *Struktura Vodnykh Rastvorov Elektrolitov i Gidratatsiya Ionov*. Moscow: Acad. Sci. USSR
68. Sharp KA, Nicholls A, Fine RF, Honig B. 1991. Reconciling the magnitude of the microscopic and macroscopic hydrophobic effects. *Science* 252:106–9
69. Shiratani E, Sasai M. 1998. Molecular scale precursor of the liquid-liquid phase transition of water. *J. Chem. Phys.* 108:3264–76
70. Silverstein KAT, Dill KA, Haymet ADJ. 1998. Hydrophobicity in a simple model of water: solvation and hydrogen bond energies. *Fluid Phase Equilibria* 150–151:83–90
71. Silverstein KAT, Dill KA, Haymet ADJ. 2001. Hydrophobicity in a simple model of water. Entropy penalty as a sum of competing terms via full, angular expansion. *J. Chem. Phys.* 114:6303–14
72. Silverstein KAT, Haymet ADJ, Dill KA. 1998. A simple model of water and the hydrophobic effect. *J. Am. Chem. Soc.* 120:3166–75
73. Silverstein KAT, Haymet ADJ, Dill KA. 1999. Molecular model of hydrophobic solvation. *J. Chem. Phys.* 111:8000–9
74. Silverstein KAT, Haymet ADJ, Dill KA. 2000. The strength of hydrogen bonds in liquid water and around nonpolar solutes. *J. Am. Chem. Soc.* 122:8037–41
75. Smith WR, Nezbeda I. 1984. Cluster expansions for hydrogen-bonded fluids. III. Water. *J. Chem. Phys.* 81:3694–99
76. Southall NT, Dill KA. 2000. The mechanism of hydrophobic solvation depends on solute radius. *J. Phys. Chem. B* 104:1326–31
77. Southall NT, Dill KA. 2001. Response to "Comment on "The mechanism of hydrophobic solvation depends on solute radius," J. Phys. Chem. B, 2000, 104, 1326." *J. Phys. Chem. B* 105:2082–83
78. Southall NT, Dill KA, Haymet ADJ. 2002. The view of the hydrophobic effect. *J. Phys. Chem. B* 106:521–33
79. Speedy RJ, Angell CA. 1976. Isothermal compressibility of supercooled water and evidence for a thermodynamic singularity at −45°C. *J. Chem. Phys.* 65:851–58
80. Sprik M, Huttel J, Parrinello M. 1996. Ab initio molecular dynamics simulation of liquid water: comparison of three gradient-corrected density functionals. *J. Chem. Phys.* 105:1142–52
81. Sprik M, Klein ML. 1988. A polarisable model for water using distributed charge sites. *J. Chem. Phys.* 89:7556–60
82. Stillinger FH. 1975. Theory and molecular models for water. *Adv. Chem. Phys.* 31:1–102
83. Stillinger FH. 1980. Water revisited. *Science* 209:451–57
84. Stillinger FH, Rahman A. 1974. Improved simulation in liquid water by molecular dynamics. *J. Chem. Phys.* 60:1545–57
85. Tait MJ, Franks F. 1971. Water in biological systems. *Nature* 230:91
86. Tanford C. 1979. Interfacial free energy and the hydrophobic effect. *Proc. Natl. Acad. Sci. USA* 76:4175–76
87. Tanford C. 1980. *The Hydrophobic Effect: Formation of Micelles and Biological Membranes*. New York: Wiley
88. Truskett TM, Debenedetti PG, Sastry S, Torquato S. 1999. A single-bond approach to orientation-dependent interactions and its implications for liquid water. *J. Chem. Phys.* 111:2647–56
89. Truskett TM, Debenedetti PG, Torquato S. 1999. Thermodynamic implications of confinement for a water-like fluid. *J. Chem. Phys.* 114:2401–18
90. Truskett TM, Dill KA. 2002. A simple statistical mechanical model of water. *J. Phys. Chem. B* 106:11829–42
91. Truskett TM, Dill KA. 2002. Predicting water's phase diagram and liquid-state anomalies. *J. Chem. Phys.* 117:5101–4
92. Truskett TM, Dill KA. 2003. A simple analytical model of water. *Biophys. Chem.* 105:449–59

93. Urbič T, Vlachy V, Kalyuzhnyi YV, Dill KA. 2003. Orientation-dependent integral equation theory for a two-dimensional model of water. *J. Chem. Phys.* 118:5516–25
94. Urbič T, Vlachy V, Kalyuzhnyi YV, Southall NT, Dill KA. 2000. A two-dimensional model of water: theory and computer simulations. *J. Chem. Phys.* 112: 2843–48
95. Urbič T, Vlachy V, Kalyuzhnyi YV, Southall NT, Dill KA. 2002. A two-dimensional model of water: solvation of nonpolar solutes. *J. Chem. Phys.* 116:723–29
96. Wertheim MS. 1986. Fluids with highly directional attractive forces. III. Multiple attraction sites. *J. Stat. Phys.* 42:459–77
97. Wertheim MS. 1987. Thermodynamic perturbation theory of polymerization. *J. Chem. Phys.* 87:7323–31
98. Zhu SB, Singh S, Robinson GW. 1994. Field-perturbed water. *Adv. Chem. Phys.* 85:627–731

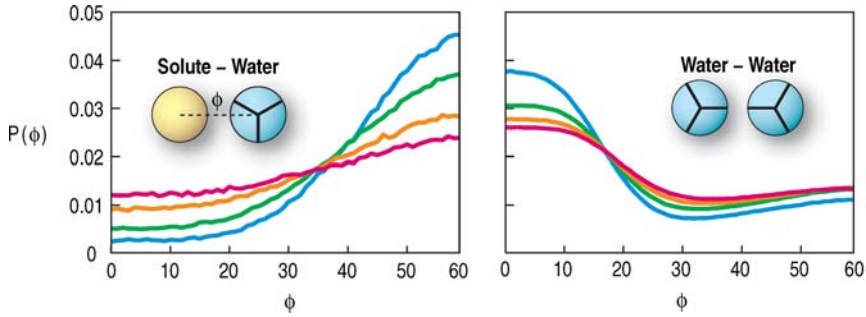

Figure 6 Angular distributions of first-shell (*left panel*) and second-shell (*right panel*) water molecules around a nonpolar solute compared with the neighbors of bulk water molecules at four temperatures: $T^* = 0.16$ (*blue*), 0.20 (*green*), 0.24 (*orange*), and 0.28 (*red*) (72).

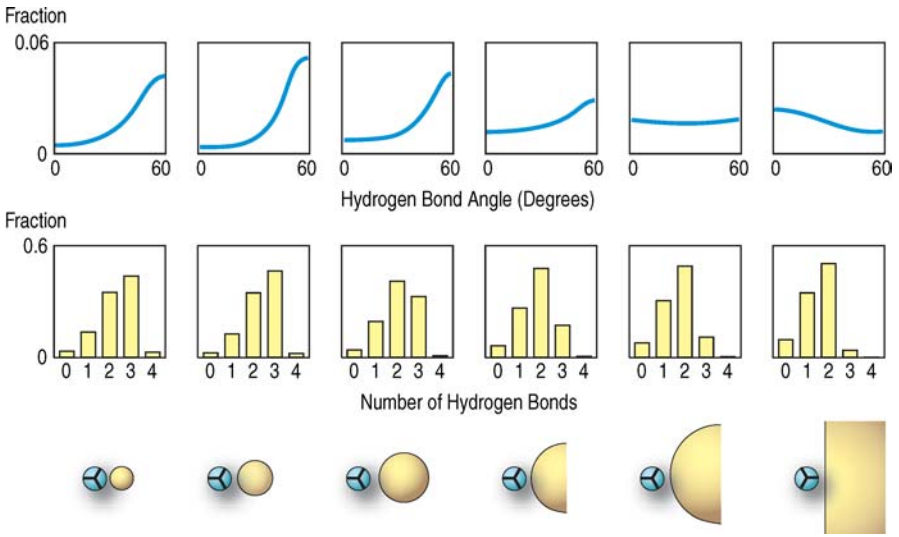

Figure 7 Angular preferences of the first-shell waters, percentage of hydrogen bonds made, and solute size (relative to an MB water) for solutes of size $0.70l_{HB}$, $1.07l_{HB}$, $1.50l_{HB}$, $2.00l_{HB}$, $3.00l_{HB}$, and a planar solute, at $T^* = 0.18$ (76).

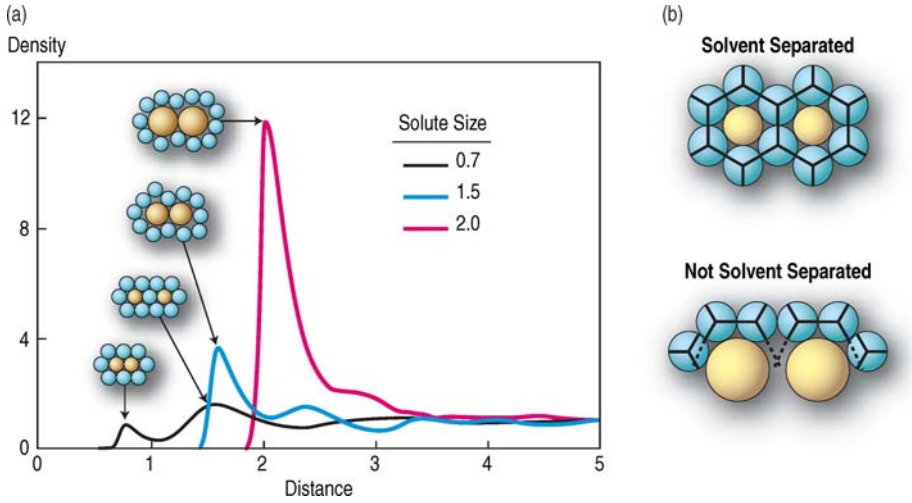

Figure 9 (*a*) Solute-solute pair distribution functions from the MB model for different solute sizes. (*b*) Small nonpolar solutes prefer to be solvent separated; large nonpolar solutes prefer to come into contact.

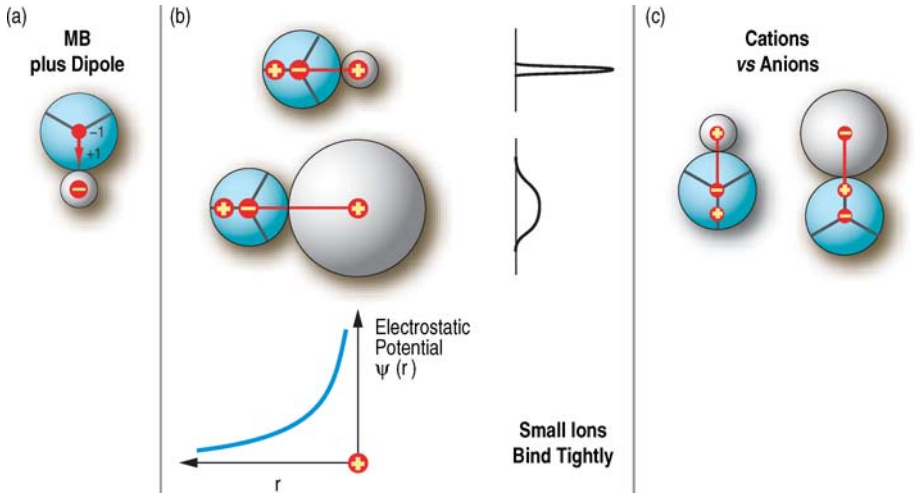

Figure 11 (*a*) The MB + dipole model of water. The negative end of the dipole is at the molecular center, and the positive end is along one hydrogen bond arm, 60% of the way to water's surface. (*b*) Smaller ions interact more strongly with water than larger ions do owing to the monotonic decrease with distance of electrostatic interactions. The distributions on the right indicate the degree of orientational freedom due to electrostatic interactions. (*c*) Anions interact more strongly with water than cations do, for a given ion radius, owing to the asymmetry of water's dipole.

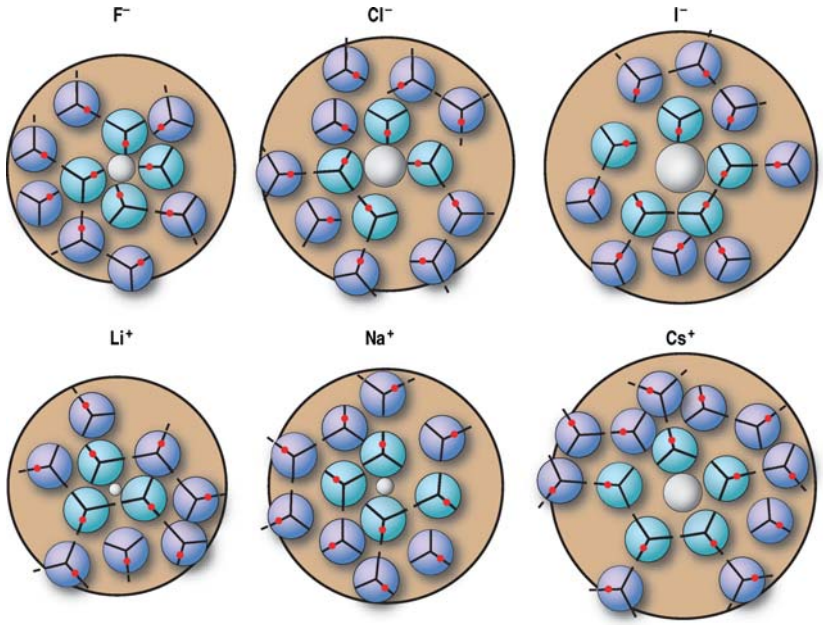

Figure 12 Snapshots of waters around ions of different sizes. Around small ions, waters are ordered electrostatically by their dipole orientations. Around large ions, waters are ordered to achieve hydrogen bonding, as around hydrophobic solutes (41). The red dots on the waters show the + end of the dipole; the – end is at the water's center.

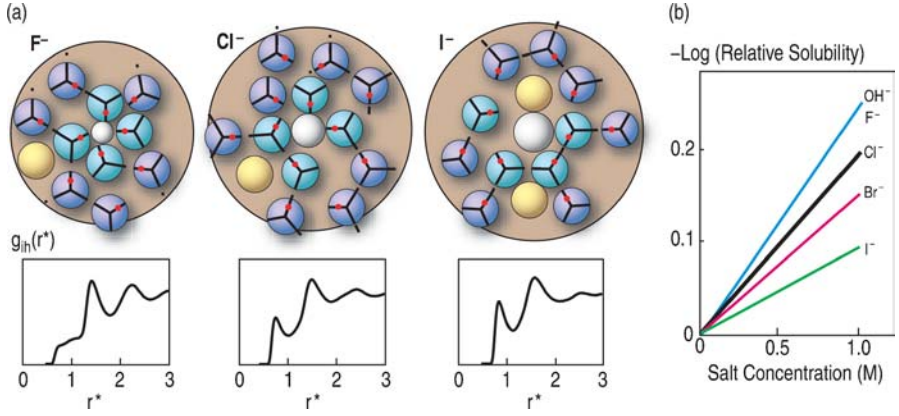

Figure 13 (*a*) Most probable sites of hydrophobic solute insertion (*yellow*) in the first and second shells around different ions, as predicted by the MB + dipole model, together with the potential of mean force between an ion and a hydrophobe at $T^* = 0.20$ (41). (*b*) Hofmeister effect: Benzene is increasingly insoluble in water of increasing ion concentrations, depending on the ion type (52).

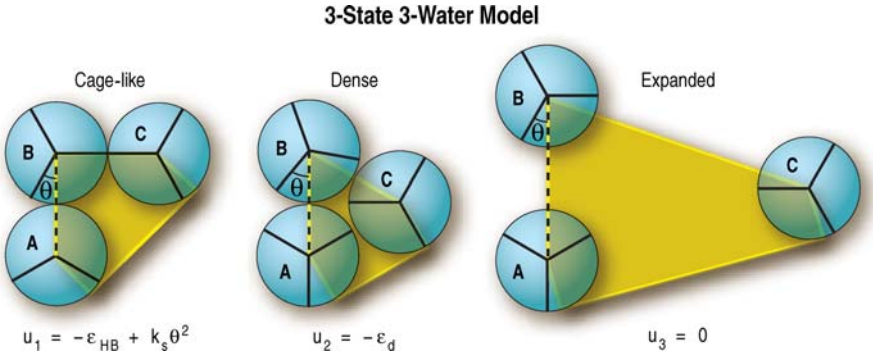

Figure 14 The three-state three-water (3S3W) model. State 1: cage-like; State 2: dense; State 3: expanded. Volumes v_j ($j = 1, 2, 3$) are computed using house-shaped cells (91) (*shaded*). The house volume sums to $\pi d^2/4$; i.e., one total water molecule per cell, plus free volume. In the cage-like state, B–C is hydrogen bonded, modulated by the angle with A–B. In the dense state, A, B, and C are in van der Waals contact, and B's orientation is not constrained by hydrogen bonds. The expanded state has neither hydrogen bonds nor van der Waals contacts. B's orientation θ is measured with respect to the axis connecting the centers of A and B.

Annual Review of Biophysics and Biomolecular Structure
Volume 34, 2005

CONTENTS